Received: 10 May 2024 | Revised: 3 September 2024 | Accepted: 6 September 2024

DOI: 10.1002/pld3.70006

RESEARCH ARTICLE

Arabidopsis apoplast TET8 positively correlates to leaf senescence, and *tet3tet8* double mutants are delayed in leaf senescence

Jayde A. Zimmerman[1] | Benjamin Verboonen[2] | Andrew P. Harrison Hanson[3] | Luis R. Arballo[4] | Judy A. Brusslan[5]

[1]Southern California Coastal Water Research Project, Costa Mesa, California, USA

[2]University of California, Riverside, Riverside, California, USA

[3]Burrell College of Osteopathic Medicine, Melbourne, Florida, USA

[4]California State University, Long Beach, Long Beach, California, USA

[5]Department of Biological Sciences, California State University, Long Beach, Long Beach, California, USA

Correspondence
Judy A. Brusslan, Department of Biological Sciences, California State University, Long Beach, Long Beach, California, USA.
Email: judy.brusslan@csulb.edu

Funding information
Andrew P. Harrison Hanson was funded by the NIH (NIGMS) RISE program R25GM071638. Luis R Arballo was funded by the CSU-LSAMP (NSF-California State University) Program (HRD-1302873). Judy A Brusslan was funded by numerous Small Faculty Grants from California State University Long Beach.

Abstract

Extracellular vesicles (EVs) are membrane-bound exosomes secreted into the apoplast. Two distinct populations of EVs have been described in Arabidopsis: PEN1-associated and TET8-associated. We previously noted early leaf senescence in the *pen1* single and *pen1pen3* double mutant. Both PEN1 and PEN3 are abundant in EV proteomes suggesting that EVs might regulate leaf senescence in soil-grown plants. We observed that TET8 is more abundant in the apoplast of early senescing *pen1* and *pen1pen3* mutant rosettes and in older wild-type (WT) rosettes. The increase in apoplast TET8 in the *pen1* mutant did not correspond to increased *TET8* mRNA levels. In addition, apoplast TET8 was more abundant in the early leaf senescence *myb59* mutant, meaning the increase in apoplast TET8 protein during leaf senescence is not dependent on *pen1* or *pen3*. Genetic analysis showed a significant delay in leaf senescence in *tet3tet8* double mutants after 6 weeks of growth suggesting that these two tetraspanin paralogs operate additively and are positive regulators of leaf senescence. This is opposite of the effect of *pen1* and *pen1pen3* mutants that show early senescence and suggest PEN1 to be a negative regulator of leaf senescence. Our work provides initial support that apoplast-localized TET8 in combination with TET3 positively regulates age-related leaf senescence in soil-grown Arabidopsis plants.

1 | INTRODUCTION

Extracellular vesicles (EVs) are secreted vesicles surrounded by one or more lipid bilayers produced by bacteria, archaea, fungi, animals, and plants (Bose et al., 2020; Chaya et al., 2024; Dai et al., 2020; Liebana-Jordan et al., 2021). Heterogenous EVs are broadly divided into three categories based on size and biogenesis. Exosomes range from 50 to 150 nm and form as intraluminal vesicles in multivesicular bodies (MVBs), ectosomes (50–1000 nm) pinch off from the plasma membrane, and apoptotic bodies (50–5000 nm) form during plasma membrane blebbing. Exosomes play many roles in intercellular signaling within the mammalian tumor microenvironment and in young and aging cells (Lananna & Imai, 2021).

Plant EVs were first noted in barley epidermal cells inoculated with biotrophic fungi. Outward budding paramural bodies were observed by transmission electron microscopy. The paramural bodies

localized to the site of cell wall appositions that slowed fungal penetration and stained for H_2O_2 and the PRX7 vacuolar peroxidase, suggesting a role in reactive oxygen species (ROS)-related cell wall defense (An, Ehlers, et al., 2006; An, Huckelhoven, et al., 2006).

Plant EVs were later purified from apoplast fluid by differential centrifugation (Cai et al., 2018; Regente et al., 2009; Rutter & Innes, 2017). The two most studied plant EVs are described as PEN1-associated and TET8-associated. Both PEN1 and TET8 are plasma membrane proteins. PEN1, also known as SYP121, is a syntaxin while TET8 is a member of the tetraspanin family, a protein component shared with animal exosomes. Tetraspanins CD63, CD81, and CD9 are abundant in purified mammalian exosomes (Jeppesen et al., 2019). Both PEN1 and TET8 are found in plant EVs. PEN1-associated EVs are enriched after a 40,000 $\times g$ centrifugation and estimated to be 150 nm in diameter (Rutter & Innes, 2017). TET8-associated EVs show enrichment after 100,000 $\times g$ centrifugation (He et al., 2021). Arabidopsis expressing mCherry-PEN1 and TET8-GFP show two non-overlapping EV populations, but differential centrifugation does not entirely separate these two classes of EVs (He et al., 2021). In addition, the two EV populations may have distinct biogenesis pathways as revealed by partial overlap of TET8-YFP with the MVB marker ARA6-CFP, but no overlap between ARA6-YFP and CFP-PEN1 (Cai et al., 2018; He et al., 2021). However, the PEN1-enriched EV proteome does share components with the ARA6 subcellular proteome (Heard et al., 2015).

The first EV proteome was determined from iodixanol density-gradient purified vesicles (Rutter et al., 2017). Proteins related to defense, ROS, membrane trafficking, vesicle transport, and ion transport were identified. A second EV proteome also harbored defense and stress response proteins (He et al., 2021). PEN1 and TET8 were detected in the two proteomes, and in both cases, PEN1 was more abundant. Both proteomes had high peptide counts for PEN3, an ABC transporter protein with specificity for defense-related indole-metabolites such as camalexin (He et al., 2019; Lu et al., 2015). The sorghum EV proteome shares many Arabidopsis EV proteins suggesting EV conservation between monocots and dicots (Chaya et al., 2024).

mRNAs reside inside EVs, and two of these, *SAG21* and *APS1*, are transferred to biotrophic fungal cells, where they are translated and contribute to reduced fungal infectivity (Wang et al., 2024). Other EV-resident RNAs are tiny RNAs (10–17 nucleotides) from coding sequences, transposable elements, and intergenic regions. The tiny RNAs are mostly derived from the middle of cellular RNAs and likely represent degradation products that remain after 5′ and 3′ exonuclease digestion (Baldrich et al., 2019). Trypsin and RNase A digestion were performed to remove protein-bound RNA co-purifying with EVs. After this treatment, only seven miRNAs were shown to be EV resident with six of these being passenger strands. The function of the EV-resident tiny RNAs and miRNAs has not been determined (Zand Karimi et al., 2022).

Additional genetic analysis suggests that EVs play a role in defense. PEN1 enhances defense against fungal haustorium penetration (Collins et al., 2003) and is thought to facilitate vesicle formation for cell wall reinforcement. *tet8tet9* double mutants are more susceptible to *Botrytis cinerea* infection, displaying larger lesions than WT (Cai et al., 2018). In contrast, *tet8* mutants are less responsive to the defense hormone salicylic acid (SA) showing reduced ROS production and cell death (Liu et al., 2020). *tet8* mutants retain ~40% of EVs; this partial reduction in EVs could be explained by PEN1-associated EVs or EVs with other tetraspanins. *TET9* is the closest paralog of *TET8*, but it is expressed at low levels under the standard growth conditions used in the Liu et al. (2020) study. *TET3* is in a sister clade to *TET8* and is highly expressed (Figure S1). *TET3* expression is abscisic acid (ABA), drought and cold-responsive (Wang et al., 2015), and TET3 may be able to form EVs in *tet8* mutants.

We have previously reported that the *pen1pen3* double mutant displays early SA-dependent leaf senescence (Crane et al., 2019). Leaf senescence is the gradual dismantling of older leaves that maximizes nutrient export prior to leaf death. Both PEN1 and PEN3 are abundant EV proteins suggesting that EVs may play a role in leaf senescence. In addition, SA has been shown to increase PEN1-associated EVs (He et al., 2021; Rutter & Innes, 2017), and age-induced leaf senescence is regulated by SA (Buchanan-Wollaston et al., 2005). To provide evidence supporting a role for EVs in leaf senescence, we have quantified TET8 in apoplast fluid as an approximation of TET8-associated EVs. We note that TET8 signal is increased in the early senescent *pen1* and *pen1pen3* and in older WT rosettes. Apoplast TET8 is dramatically increased in older rosettes of *pen1* mutants, but not in younger rosettes, suggesting that apoplast TET8 is not compensating for loss of PEN1 but is associated with leaf senescence. Additionally, apoplast TET8 is increased in the early-senescent *myb59* mutant (He et al., 2023). Beyond correlation, *tet3tet8* double mutants show a significant delay in leaf senescence, and the early leaf senescence displayed by *pen1* mutants is reversed in *pen1tet3* and *pen1-tet8*. Our apoplast TET8 and genetic data point to opposing roles for PEN1 and two tetraspanins (TET3 and TET8) in leaf senescence.

2 | RESULTS

2.1 | Apoplast TET8 increases in early senescing *pen1* and *pen1pen3*

We have previously reported accelerated SA-dependent leaf senescence in *pen1pen3* mutants. PEN1 and PEN3 are abundant EV proteins suggesting that EVs may play a role in the regulation of leaf senescence. To elucidate the relationship between leaf senescence and EVs, we measured the amount of apoplast TET8 and quantified leaf senescence in WT, *pen1*, *pen3*, *pen1pen3*, and *tet8* mutants after 8 weeks of growth (Boavida et al., 2013; Collins et al., 2003; Stein et al., 2006). *tet8* served as a negative control for the TET8 antibody, and a 10-fold reduced signal was observed (Figure 1b), most likely due to other TET homologs (Figure S1). A significantly brighter apoplast TET8 signal was observed in the *pen1* and *pen1pen3* mutants compared to the wild-type and the *pen3* mutant (Figures 1a,b, S2). TET8 was enriched in apoplast fluid, and not consistently detectable in

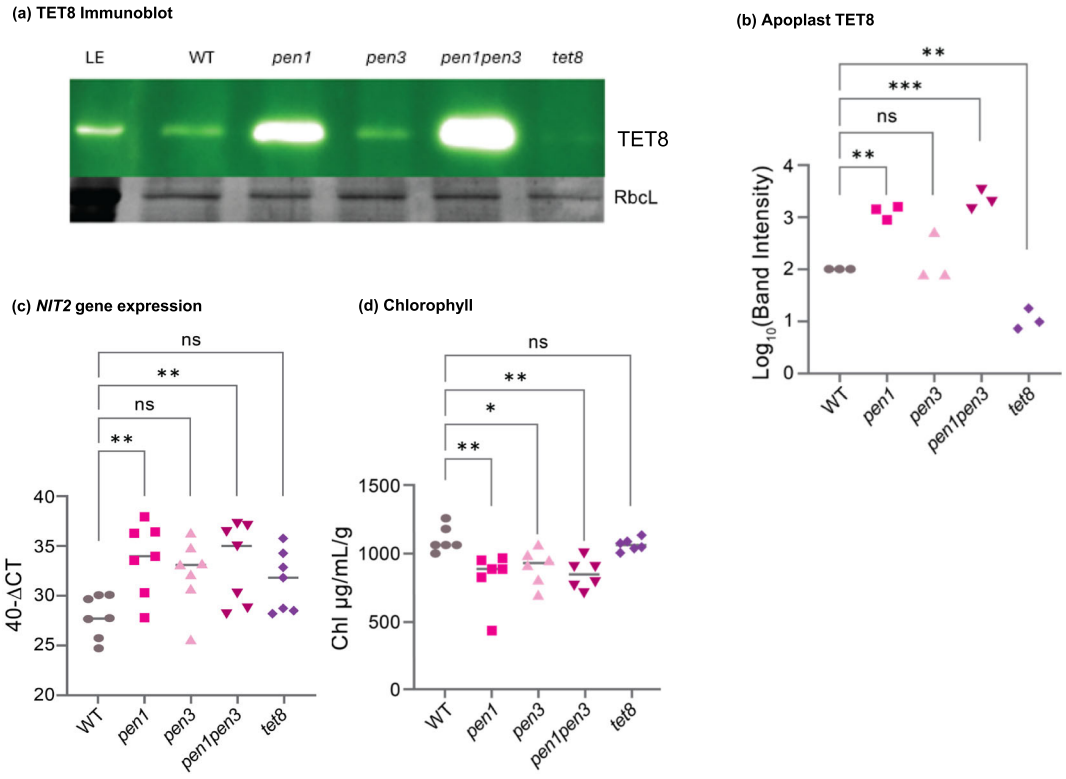

FIGURE 1 Apoplast TET8 increases in early leaf senescence mutants *pen1* and *pen1pen3*. (a) TET8 was detected in leaf extract (LE) from wild-type (WT) and apoplast fluid from WT, *pen1*, *pen3*, *pen1pen3*, and *tet8* using an immunoblot normalized to Coomassie-stained RbcL. TET8 antibody verification on uncropped immunoblots shown in Figure S3. (b) Normalized TET8 chemiluminescent signals from three independent experimental replicates are shown. (c) From the same 8-week-old tissue, Leaves 4 and 5 were harvested for RNA extraction and *NIT2* gene expression, normalized to *ACT2*, was quantified. (d) Leaf 3 was harvested, and total chlorophyll was measured and normalized to fresh weight. A stronger TET8 signal in the apoplast is accompanied by higher *NIT2* expression and lower chlorophyll levels showing a positive correlation between apoplast TET8 and leaf senescence. *tet8* (SALK_136039) served as a negative control for the antibody. Additional experimental replicates are shown in Figure S2. *p*-values were reported as <.05 (*), <.01 (**), <.001 (***) and <.0001 (****). ns, not significant.

whole leaf extracts (Figure S3). The elevated apoplast TET8 (~10-fold) in *pen1* and *pen1pen3* was associated with accelerated leaf senescence. This was indicated by the significant increase in expression of the leaf senescence marker transcript *NIT2* (Figure 1c; Brusslan et al., 2012; Brusslan et al., 2015) and accompanied by significantly reduced chlorophyll (Figure 1d). Gene expression was determined from RNA isolated from Leaves 4 and 5 while chlorophyll was isolated from the older Leaf 3. Rosette leaves are numbered according to emergence from the meristem with Leaf 1 emerging first (Figure S4). Specific rosette leaves allowed comparison between leaves of similar age, and since chlorophyll loss occurs after increases in *NIT2* gene expression, the slightly older leaves were used for chlorophyll measurements. Taken together, our results suggest that *pen1* and *pen1-pen3* mutants have elevated levels of apoplast TET8 correlating to accelerated leaf senescence.

2.2 | Apoplast TET8 increases with plant age

To support the correlation between early leaf senescence and apoplast TET8, we next determined if the progression of leaf senescence in WT was associated with an increase in apoplast TET8. We collected apoplast fluid from WT rosettes at different ages and isolated RNA and chlorophyll from the same plants (Figures 2, S5). Older rosettes (8 weeks) presented a significant increase in apoplast TET8 (~3-fold) compared to 5-week-old plants (Figure 2a,b). The rosettes were undergoing leaf senescence shown by increased *NIT2* expression (Figure 2c) and a reduction in chlorophyll (Figure 2d). Older rosette leaves were used for chlorophyll (Leaf 3) and *NIT2* gene expression (Leaves 4 and 5) while whole rosettes were used to provide sufficient starting material for apoplast extraction, which may explain why significant changes in leaf senescence markers (6 weeks) occurred earlier than increased apoplast TET8 (8 weeks). These results show that apoplast TET8 increases during the progression of age-related leaf senescence.

2.3 | Apoplast TET8 is increased in *pen1* mutants only during leaf senescence

Leaves contain both PEN1-associated and TET8-associated EVs, and loss of PEN1 in the *pen1* mutant could be compensated by an increase

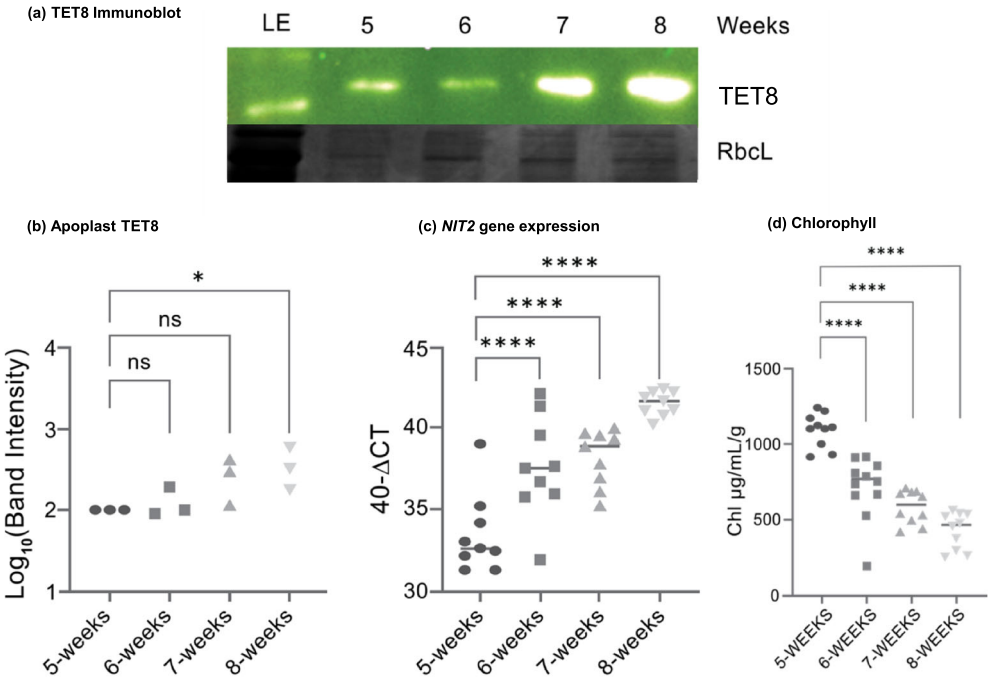

FIGURE 2 An increase in apoplast TET8 was observed in older wild-type (WT) rosettes. (a) Apoplast TET8 was detected from rosettes harvested at 5 to 8 weeks using an immunoblot normalized to Coomassie-stained RbcL. (b) Normalized TET8 chemiluminescent signals from three independent experimental replicates are shown. (c) *NIT2* gene expression (Leaves 4 and 5) and (d) chlorophyll (Leaf 3) are shown from plants grown alongside those used for apoplast extraction. Additional experimental replicates are shown in Figure S3. *p*-values were reported as <.05 (*), <.01 (**), <.001 (***) and <.0001 (****). ns, not significant.

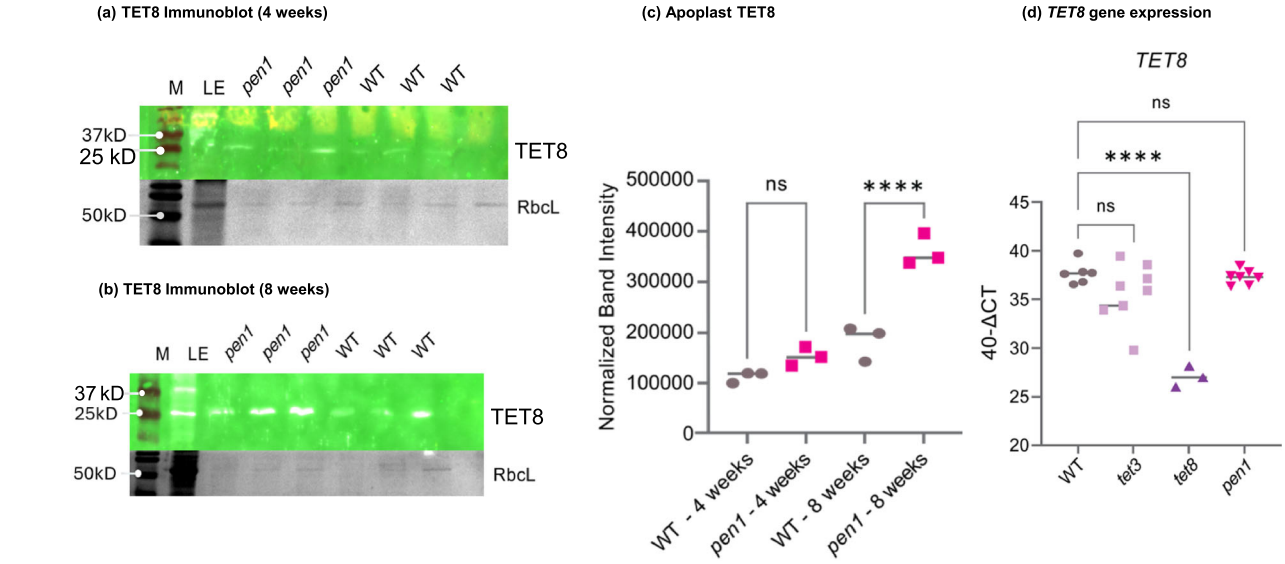

FIGURE 3 Apoplast TET8 is more abundant in *pen1* mutants during leaf senescence but not in younger rosettes. (a) Apoplast was extracted from wild-type (WT) and *pen1* rosettes after 4 weeks (a) or 8 weeks (b) and subject to immunoblot analysis and normalization with Coomassie-stained RbcL. Three experimental replicates at each age are shown in the immunoblot. (c) Normalized TET8 chemiluminescent signal from the three replicates is shown, and the significant difference after 8 weeks of growth between WT and *pen1* is evident. (d) *TET8* gene expression, normalized to *ACT2*, was measured by real-time quantitative polymerase chain reaction (RT-qPCR) in Leaves 4 and 5 from 8-week-old plants. *TET8* mRNA levels were unchanged in WT, *tet3* (SAIL_617_C05), and *pen1*, but partial transcripts were reduced 1000-fold (2^-10) in *tet8*. *p*-values were reported as <.05 (*), <.01 (**), <.001 (***) and <.0001 (****). ns, not significant.

in TET8-associated EVs, independent of leaf senescence. To explore this possibility, apoplast was isolated from ~4 g of 4-week (non-senescent) and 8-week-old (senescent) WT and *pen1* rosettes. Apoplast TET8 is minimally and equally abundant in WT and *pen1* at 4 weeks, but significantly more abundant (~2-fold) in *pen1* at 8 weeks (Figure 3a–c, each sample is an independent experimental replicate). The increase in apoplast TET8 is not accompanied by an increase in *TET8* gene expression (Figure 3d) demonstrating that *TET8* mRNA levels do not directly reflect apoplast TET8 abundance. These findings show that apoplast TET8 does increase in *pen1* during leaf senescence, but not before, and that this change does not occur at the level of gene expression. As *pen1* displays earlier leaf senescence, these findings also support the positive relationship between apoplast TET8 and leaf senescence.

2.4 | Apoplast TET8 is increased in the early senescing *myb59* mutant

We were concerned that early senescence in *pen1* and *pen1pen3* might complicate our experiments since PEN1 and PEN3 are EV-resident proteins. Hence, we measured apoplast TET8 in an early leaf senescence mutant that was not in a gene encoding an EV component. We obtained the *myb59* allele (GABI-KAT_627C09, He et al., 2023) and observed accelerated leaf senescence when plants were transferred to higher light intensity for the last 3 weeks of the 6-week growth period (Figure 4a). Chlorophyll was significantly decreased, and *NIT2* gene expression was significantly increased in *myb59*. Early leaf senescence was not observed when *myb59* remained in lower light intensity. Apoplast fluid was similarly extracted from WT and *myb59* (both grown together under the same light conditions), and Figure 4b,c shows that apoplast TET8 was increased ~6-fold in the early senescing *myb59* in three separate experiments. This supports a positive correlation between leaf senescence and apoplast TET8 accumulation that is not related to perturbation of *pen1*/*pen3*.

2.5 | Genetic analysis indicates opposing roles for PEN1 and tetraspanins TET3 and TET8 in leaf senescence

Since EVs are identified as PEN1-associated and TET8-associated, we generated a *pen1tet8* mutant to reduce EV production. We noted that *TET3* is reported to be induced by leaf senescence and its expression level is similar to *TET8* (Figures S1, 3d and S6). Although TET3 is not observed in any EV proteome, its abundance and similarity to TET8 suggest that it may have related functions. For this reason, we also produced *pen1tet3* and *tet3tet8* double mutants. The *tet3* T-DNA mutant allele was shown to be a strong knockdown (Figure S6). Plants were grown for 6 weeks, and chlorophyll and *NIT2* gene expression were used to quantify leaf senescence (Figure 5). Six weeks was chosen to reduce variability encountered for longer growth times and still induce leaf senescence (Figure 2c,d). Unexpectedly, we noted that the early leaf senescence observed in *pen1* (Figure 1c,d) was reversed by *tet3* or *tet8* mutations in double mutants. In addition, the *tet3tet8* double mutant showed a marked delay in leaf senescence. These findings suggest that PEN1 and the two tetraspanins play opposite roles in leaf senescence with TET3 and TET8 promoting leaf senescence (the *tet3tet8* double mutant delays leaf senescence) and PEN1 slowing leaf senescence (the *pen1* mutant accelerates leaf senescence).

An alternative method that induces rapid leaf yellowing is dark-induced leaf senescence (DILS). Leaves are detached from the plant and incubated on filter paper in the dark, and chlorophyll levels are measured after 3 or 5 days of dark treatment. Unable to perform photosynthesis, leaves rapidly degrade chlorophyll and other macromolecules in response to starvation. The molecular pathway of DILS differs from leaf senescence in soil-grown plants (Guo & Gan, 2012; Liebsch & Keech, 2016; van der Graaff et al., 2006). We were interested in whether the double mutants would show changes in DILS and performed experiments on Leaves 1 and 2 of 3-week-old plants.

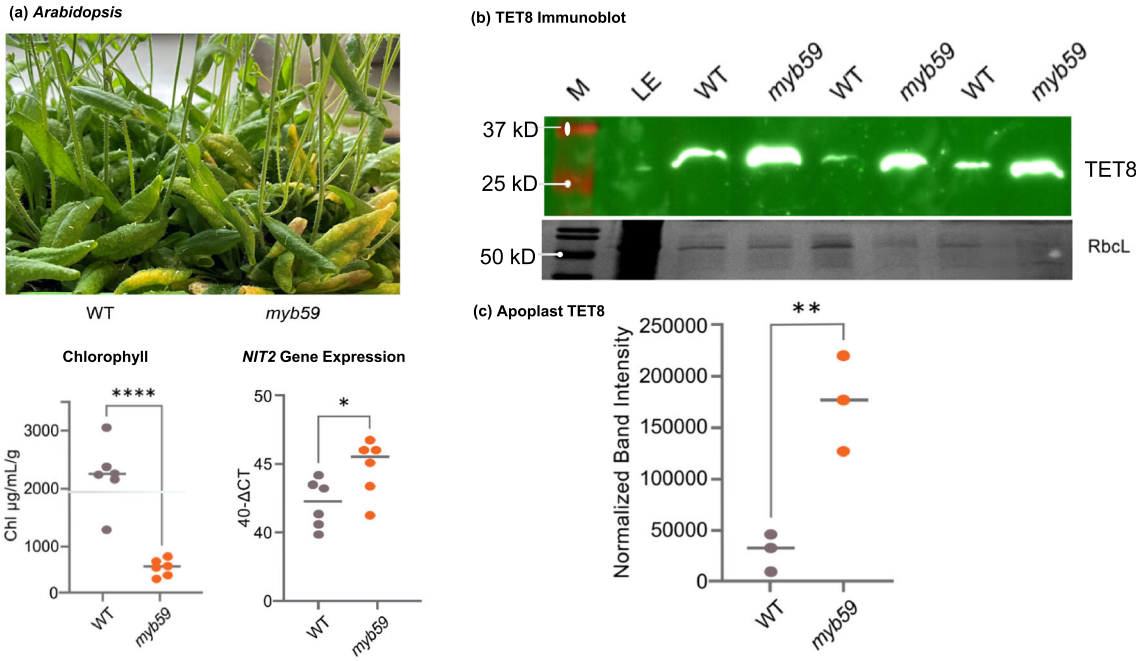

FIGURE 4 The *myb59* mutant displays early leaf senescence and has higher apoplast TET8. (a) wild type (WT) and *myb59* were grown under long day conditions (20 h light:4 h dark) for 3 weeks at 40 µmol photons/m^2/s and then transferred to 160 µmol photons/m^2/s for three additional weeks. Reduced chlorophyll in the *myb59* line (GABI-KAT 627C09: T-DNA insertion in exon 3 of AT5G59780) is visible when compared to WT. (b) WT and *myb59* apoplast from rosette leaves was subject to TET8 immunoblot analysis. (c) Normalized TET8 chemiluminescent signal from the three independent replicates is shown, and the significant difference between WT and *myb59* is evident. *p*-values were reported as <.05 (*), <.01 (**), <.001 (***) and <.0001 (****).

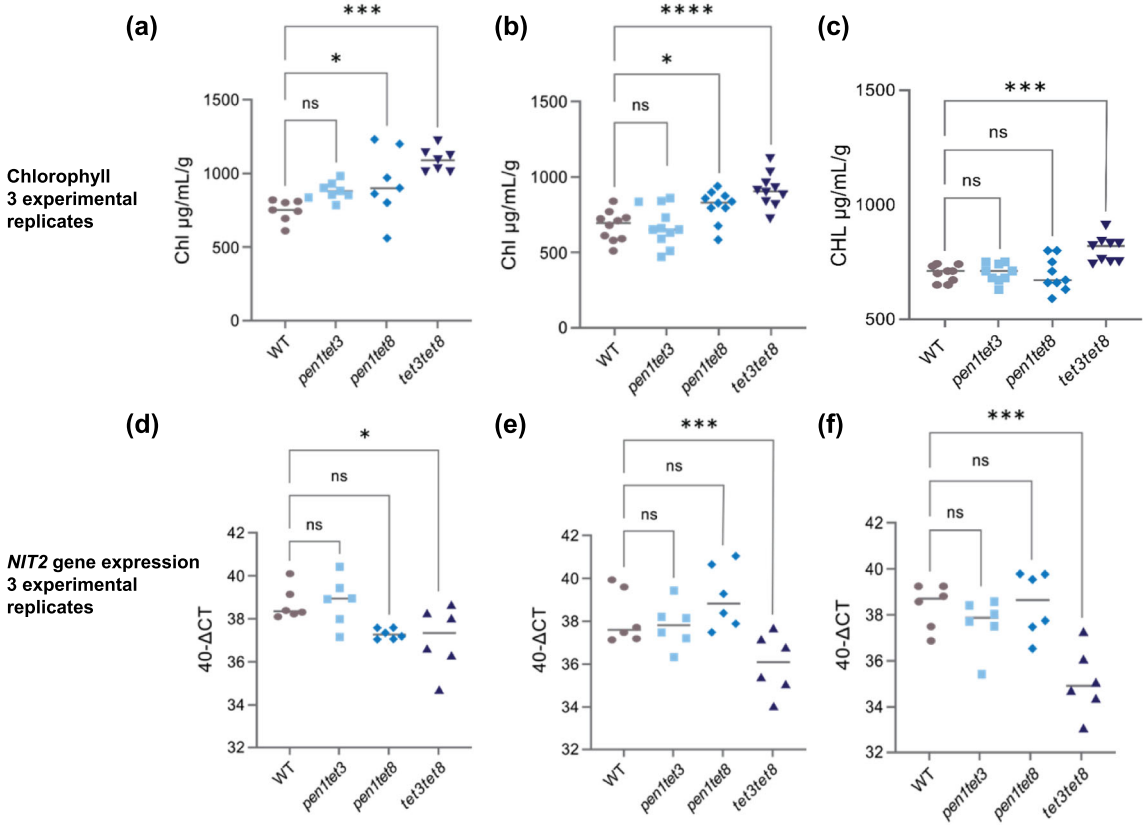

FIGURE 5 Chlorophyll and *NIT2* expression quantified after 6 weeks of growth in wild-type (WT) and double mutants. (a–c) Three independent experimental replicates showing chlorophyll levels from Leaf 3 ($n = 6$–10). (d–f) *NIT2* expression in Leaves 4 and 5 ($n = 6$). Mutations in *tet3* and *tet8* reversed the early leaf senescence observed in *pen1* while *tet3tet8* double mutants displayed a significant delay in leaf senescence. *p*-values were reported as <.05 (*), <.01 (**), <.001 (***) and <.0001 (****). ns, not significant.

The double mutants behaved similarly to WT during DILS (Figure 6), showing that the opposing roles for TET3/TET8 and PEN1 are specific to age-related leaf senescence.

3 | DISCUSSION

We have presented data that positively correlate apoplast TET8 and age-related leaf senescence. Apoplast TET8 is highly abundant in early senescing *pen1* and *pen1pen3* mutants (Figure 1), and more abundant in WT as rosettes become older (Figure 2). High levels of TET8 are not observed in pre-senescent *pen1* indicating that increased apoplast TET8 is not constitutively compensating for the loss of PEN1 (Figure 3), rather its high abundance coincides with leaf senescence. Further support for the correlation between apoplast TET8 and leaf senescence is the higher level in the early senescing *myb59* mutant (Figure 4). As SA has been shown to promote age-dependent leaf senescence and to increase EVs, these correlative data are not unexpected. Our mutant analysis provides genetic evidence supporting a causal relationship (Figure 5). We found that *tet8*, in combination with *tet3*, displayed a strong delayed senescence phenotype in soil-grown plants undergoing age-related senescence, but no change in DILS (Figure 6). This contrasts with *pen1* (and *pen1pen3*), which show early senescence. The genetic data support TET3 and TET8 promoting leaf senescence while PEN1 and PEN3 prevent leaf senescence. TET8 was previously found to be necessary for a full ROS and cell death response to SA (Liu et al., 2020), consistent with our results. Our model for these proposed roles is illustrated in Figure 7.

This work measured TET8 by immunoblot in partially purified apoplast fluid that had large vesicles and broken cells removed by a 10,000 ×***g*** spin. The apoplast was enriched for TET8 when compared to whole leaf extract. The TET8 signal likely arose from EVs, although plasma membrane fragments that formed into vesicles cannot be ruled out. Purifying EVs is challenging, and the current published Arabidopsis EV proteomes share unexpected proteins such as phototropin1 and phototropin2 (flavin-binding blue light photoreceptors, Christie, 2007) that could be EV resident or from plasma membrane micelles. Current published EV proteomes also contain contaminating chloroplast proteins (He et al., 2021; Rutter & Innes, 2017), including the notoriously abundant Rubisco large subunit. This protein was most distinct in Coomassie-stained apoplast sodium dodecyl-sulfate polyacrylamide gel electrophoresis (SDS-PAGE) and, although not the ideal candidate, was used by us and others (He et al., 2021) to compare protein amounts in apoplast samples.

When apoplast proteomes from non-senescent and senescent Arabidopsis leaves were compared, proteins related to stress-

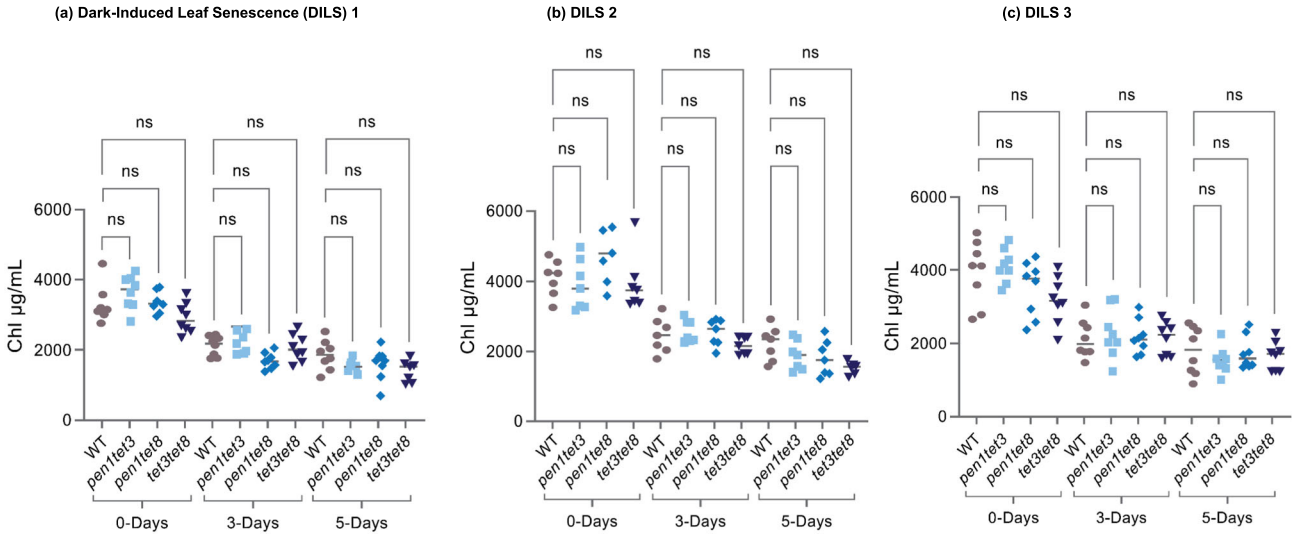

FIGURE 6 Dark-induced leaf senescence in double mutants. (a–c) Chlorophyll levels in three independent experiments using detached leaves treated in the dark for 0, 3, and 5 days ($n = 7$). There were no significant differences in chlorophyll levels at each day of dark treatment among genotypes. *p*-values were reported as <.05 (*), <.01 (**), <.001 (***) and <.0001 (****). ns, not significant.

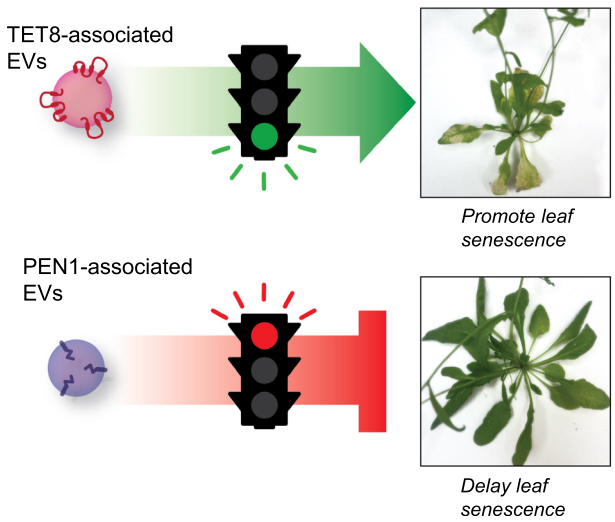

FIGURE 7 Proposed model for extracellular vesicle (EV) regulation of leaf senescence. TET8 and TET3 EVs localized in the apoplast promote leaf senescence in soil-grown plants, and *tet3tet8* double mutants show a delay in leaf senescence. PEN1-associated EVs slow leaf senescence, and *pen1* and *pen1pen3* mutants show accelerated leaf senescence. We note that we observed TET8 in partially purified apoplast and speculate it is present in EVs.

response were found to be enriched in the senescent apoplast (Borniego et al., 2020). Antifungal proteins, peroxidases, and enzymes for the catalysis of RNA were more abundant in the senescent apoplast. A few proteins that were more abundant in non-senescent leaves were shared with the EV proteome, but neither tetraspanins nor syntaxins were identified in the non-senescent or senescent apoplast proteomes. Differences in apoplast isolation (vesicle isolation buffer [VIB] vs. deionized water and differences in centrifugation steps) may account for this discrepancy.

3.1 | How might tetraspanins regulate leaf senescence?

Tetraspanins are plasma membrane and endoplasmic reticulum-localized proteins that form tetraspanin-enriched microdomains: dynamic hetero oligomeric protein platforms that regulate cell signaling, vesicle formation, and adhesion (Jimenez-Jimenez et al., 2019; Konstantinova et al., 2024; Qin et al., 2024; Reimann et al., 2017). There are 21 tetraspanins encoded by the Arabidopsis genome (Figure S1). A plant-specific domain has been noted in the large extracellular loop in TET1-TET13 (GCCK/RP) while TET14–17 and TOM2A-TOM2AH3 have GCC, VCC or YCC in this same position (Boavida et al., 2013; Fujisaki et al., 2008). TET18/TOM2AH2 was identified in one Arabidopsis EV proteome (Rutter & Innes, 2017). Since tetraspanins form heterodimers, the presence of multiple tetraspanins in EVs would be expected. Tetraspanins show variable expression in different plant tissues and in response to different stresses (Boavida et al., 2013; Qin et al., 2024; Wang et al., 2015). Genetic studies reveal roles for some tetraspanins. TET1 is important for correct auxin distribution, and *tet1* (*trn2*) mutants have abnormal cell divisions in the peripheral zone of the shoot apical meristem, disrupted cotyledon venation, severe effects on leaf development, and reduced numbers of vascular cell files in roots (Chiu et al., 2007; Cnops et al., 2006; Konstantinova et al., 2024). *tet5tet6* double mutants had larger leaves with greater numbers of cells suggesting redundant roles in attenuating cell division (Wang et al., 2015), while *tet3* mutants show reduced viral cell-to-cell movement via plasmodesmata (Zhu et al., 2022). Mutations in all four TOM2A-related tetraspanins show a severe growth defect (Fujisaki et al., 2008). Rice tetraspanin mutants show reduced height, reduced secondary branching of panicles, and lower grain yield (Qin et al., 2024). The numerous developmental and physiological roles ascribed to tetraspanins do not provide

information on mechanisms that could help define a role in regulating leaf senescence. Studies that identify TET8 and TET3 binding partners, and whether these two tetraspanins interact, may define a functional tetraspanin-enriched microdomain.

The EV lipidome is enriched in glycosyl inositol phosphoceramides (GIPCs), and TET8 binds GIPCs via its C-terminal domain (Liu et al., 2020, 2023). TET8 is proposed to facilitate EV formation by bringing GIPC-containing vesicles from the Golgi to MVBs and then to the plasma membrane for egress. Treating the *tet8* mutant with GIPCs partially restored the ROS burst in response to flg22, an elicitor of pathogen associated molecular pattern (PAMP)-triggered immunity (PTI). Further work can explore the role of GIPCs in promoting leaf senescence, which is linked to ROS production, in the *tet3tet8* double mutant.

3.2 | How might PEN1 regulate leaf senescence?

PEN1 (SYP121) is a plasma membrane syntaxin or Qa-SNARE (soluble N-ethylmaleimide-sensitive factor attachment receptor). SNAREs mediate membrane fusion by forming trans-SNARE complexes (Fujiwara et al., 2014). Proteins secreted by PEN1 act in lipid metabolism, protein folding, and cell wall modification (Waghmare et al., 2018). PEN1 localizes to detergent-resistant microdomains (Qi et al., 2011), and it interacts with annexin 4, SYP71, and a hypersensitive-induced reaction protein (HIR2, AT3G01290, Fujiwara et al., 2014). PEN1 is needed for the timely formation of the pre-invasive papillae that defend against haustorium-forming powdery mildew and rust fungi. H_2O_2-containing vesicles produced in the vicinity of pre-invasive papillae are not observed in *pen1* mutants, (Collins et al., 2003) and *pen1* mutants show greater susceptibility to initial fungal penetration. A more complete pre-invasive papillae and post-invasive encasement defense is mounted in combination with SYP122, a closely related paralog. Together, these two syntaxins mediate defense against a wider range of fungi and an oomycete (Rubiato et al., 2022). The *pen1syp122* double mutant also shows a strong auto-immune response that is reversed by mutation in *FMO1*, which blocks the synthesis of N-hydroxypipecolic acid, the mobile SA signal (Zhang et al., 2007, 2008). It is likely that early senescence in *pen1* and *pen1pen3* is related to autoimmunity since it was reversed with a *sid2* mutation, which reduces SA biosynthesis (Crane et al., 2019). The *pen1syp122* auto-immune response begins about 2 weeks after germination while the response in *pen1pen3* is weaker and commences later, after 6 weeks of growth (Crane et al., 2019; Rubiato et al., 2022). These observations support PEN1 negatively regulating leaf senescence. PEN1's prevention of leaf senescence may be more related to its auto-immunity functions, potentially through its binding to HIR2, and less related to its roles in promoting pre-invasive papillae and post-invasive encasements.

Overall, we report that apoplast TET8 positively correlates to leaf senescence and that *tet3tet8* double mutants significantly delay leaf senescence. Genetic analysis suggests that PEN1 slows leaf senescence, potentially related to its roles in autoimmunity.

4 | MATERIALS AND METHODS

4.1 | Plant growth conditions

Arabidopsis thaliana seeds were sowed in Sunshine Mix #4 soil, Sun Gro Horticulture, Agawam, MA and cold stratified at 4°C for 5 days before being grown under long-day growing conditions (20 h of light at 40 µmol photons/m^2/s, 24°C). Rosettes were supplemented every week with 10 mL of GRO POWER 4-8-2 (Gro-Power, Chino, CA) per 3.78 L of water and received an application of the larvicide, Gnatrol® (0.3 g per 400 mL), on the soil surface to prevent fungus gnats at the time of seed sowing.

4.2 | Mutants

Mutant lines used in this study are listed in Table S1. Seeds were obtained from the Arabidopsis Biological Resource Center (ABRC, Ohio State University). All plants used in these experiments were in the Col-0 ecotype. Prior to experimentation, mutations or insertions were verified by using primers designed by the iSect tool at SALK T-DNA express (http://signal.salk.edu/tdnaprimers.2.html). Flanking sequences were amplified using a T-DNA border primer and sequenced to identify the insertion site. Point mutants were identified through sequencing after amplification of the desired region. Primers are listed in Table S1.

4.3 | DNA isolation

DNA was isolated using Plant DNAzol™ (ThermFisher, Inc.) according to manufacturer's instructions. *Taq* polymerase (New England Biolabs, Inc.) was used for standard PCR reactions in a Bio-Rad T100 thermal cycler using a 57°C annealing temperature.

4.4 | Apoplast extraction

The protocol was adapted and modified from Rutter and Innes (2017) and He et al. (2021). Rosettes were harvested by cutting plants at the hypocotyl at the soil line and removing inflorescences. To provide sufficient starting material, between 5 and 10 g (approximately between 12 and 24 plants) were collected, washed in distilled water to remove soil and then submerged in 200 mL VIB (20 mM 2-(N-morphlino)ethanesulfonic acid [MES] hydrate, 2 mM $CaCl_2$, .1 M NaCl pH 6.0 with HCl) inside a 250 mL beaker. The submerged rosettes were vacuum infiltrated at −30 kPa for 30 s. The infiltrated rosettes were blotted dry and placed in 50 mL conical tubes punctured at the base. A slow-speed centrifugation (900 ×***g***, 15 min, 4 °C) was used to collect the raw apoplast (approximately 3 mL). The raw apoplast was centrifuged (2000 ×***g***, 30 min, 4°C) to pellet large cellular debris. The supernatant was transferred to autoclaved 1.5 mL microcentrifuge tubes and spun to pellet larger non-EV vesicles and broken cells (10,000 ×***g***, 30 min,

4°C). The resulting supernatant was considered partially pure apoplast that was used for immunoblotting or stored at −20°C.

4.5 | Immunoblotting

The sample preparation for whole leaf extract and SDS-PAGE protocol were adapted from Martinez-Garcia et al. (1999) with 9 µL of whole leaf extract and 1 µL of buffer Z per lane. Fourteen microliters of apoplast and 4 µL of 4× loading buffer (250 mM Tris–HCl, pH 6.8, 10% SDS, 30% glycerol, 10 mM dithiothreitol (DTT), 0.05% bromophenol blue) were denatured at 95°C prior to electrophoresis. After electrophoresis, protein was transferred to nitrocellulose using a Bio-Rad Transblot Turbo Transfer system. Immunoblotting was performed using the TET8 antibody (PhytoAB PHY1490S, lot# 1941A5) and the goat anti-rabbit horseradish peroxidase (HRP) secondary antibody (PhytoAB PHY600, lot #2206A5). HRP was detected with Super Signal™ West Pico PLUS (ThermoFisher, Inc.). Relative protein present in each sample was quantified with Coomassie brilliant blue dye using the most prominent band: RbcL. TET8 signal was normalized based on relative protein amount. Imaging for HRP detection and Coomassie staining was performed with a ProteinSimple FluorChem Fluorescent Western Blot Imaging System.

4.6 | Real-time quantitative polymerase chain reaction (qPCR)

Leaves 4 and 5 were harvested from an individual plant for each sample (Figure S4). The number of samples for each condition varied from 6 to 10. Leaves were transferred to a 1.5 mL tube, frozen in liquid nitrogen, and stored at −80°C. RNA was isolated using Trizol, and cDNA was synthesized using MuMLV reverse transcriptase (New England Biolabs, Inc.) primed with random hexamers. *ACT2*, *NIT2*, and *TET* primers (Table S1) at 70 nM with 1× SYBR Green (qPCRBIO SyGreen, Blue Mix Lo-ROX, PCR Biosystems) were used to amplify a 1:16 dilution of cDNA in triplicate in a Quantstudio™6 PRO real-time thermal cycler (ThermoFisher, Inc.) with a 61°C annealing temperature. *NIT2* or *TET* gene expression normalized to *ACT2* was calculated (40-ΔCt; Garapati et al., 2015; Livak & Schmittgen, 2001).

4.7 | Chlorophyll

Leaf 3 was harvested for each sample (Figure S4). The number of samples for each condition varied from 6 to 10. Each leaf was weighed, transferred to a 1.5 mL tube, frozen in liquid nitrogen, and stored at −80°C.The number of samples varied from 6 to 10. Leaves were submerged in 800 µL dimethylformamide (DMF) upon thawing, and chlorophyll was eluted into the DMF in the dark at room temperature for 16–24 h. Absorbance was measured at 647 and 664 nm, and chlorophyll concentrations were calculated using equations described in Porra et al. (1989) and normalized to leaf weight.

4.8 | DILS

Leaves 3 and 4 were collected from plants after 21 days of growth. Leaves 3 and 4 emerge from the meristem close to the same time and are nearly equal in age and size at 21 days. Leaves were flash frozen (Day 0) or arranged on filter paper (Whatman Hardened Ashless 125 mm) saturated with 1.5 mL of 3 mM MES (pH 5.8) and adhered to a petri dish. Petri dishes were sealed with parafilm and then placed in dark canisters in the growth chamber. Dark canisters were removed after 3 or 5 days, and leaves were flash frozen in 1.5 mL tubes and stored at −80°C prior to chlorophyll measurements. Samples were not normalized to weight as the size of the leaves was uniform.

4.9 | Statistical analysis

All statistical analyses were performed in GraphPad Prism. Outliers were removed using default parameters, and log normality was verified prior to analyses. In some instances, data were log transformed prior to statistical analysis. Different experimental conditions were compared to the control using a one-way ANOVA with Dunnett's correction for multiple comparisons. For experiments with two conditions, a *t*-test was used to determine if the difference was significant. *p*-Values were reported as <.05 (*), <.01 (**), <.001 (***) and <.0001 (****). ns = not significant.

AUTHOR CONTRIBUTIONS

Jayde A. Zimmerman, Benjamin Verboonen, Andrew P. Harrison Hanson, Luis R. Arballo, and Judy A. Brusslan designed and performed the research and analyzed data. Jayde A. Zimmerman and Judy A. Brusslan wrote the paper.

ACKNOWLEDGMENTS

The authors wish to thank our funding sources, the CSULB Science Shop, and Thomas Douglass for computer support.

CONFLICT OF INTEREST STATEMENT

The Authors did not report any conflict of interest.

DATA AVAILABILITY STATEMENT

Mutant lines generated by this work will be submitted to the Arabidopsis Biological Resource Center.

ORCID

Jayde A. Zimmerman https://orcid.org/0009-0002-1540-4991
Benjamin Verboonen https://orcid.org/0009-0003-6540-2174
Luis R. Arballo https://orcid.org/0009-0001-1576-5298
Judy A. Brusslan https://orcid.org/0000-0002-6744-3696

REFERENCES

An, Q., Ehlers, K., Kogel, K. H., Van Bel, A. J. E., & Hückelhoven, R. (2006). Multivesicular compartments proliferate in susceptible and resistant MLA12-barley leaves in response to infection by the biotrophic

powdery mildew fungus. *New Phytologist*, *172*, 563–576. https://doi.org/10.1111/j.1469-8137.2006.01844.x

An, Q., Huckelhoven, R., Kogel, K.-H., & van Bel, A. J. E. (2006). Multivesicular bodies participate in a cell wall-associated defence response in barley leaves attacked by the pathogenic powdery mildew fungus. *Cellular Microbiology*, *8*, 1009–1019. https://doi.org/10.1111/j.1462-5822.2006.00683.x

Baldrich, P., Rutter, B. D., Karimi, H. Z., Podicheti, R., Meyers, B. C., & Innes, R. W. (2019). Plant extracellular vesicles contain diverse small RNA species and are enriched in 10- to 17-nucleotide "tiny" RNAs. *The Plant Cell*, *31*, 315–324. https://doi.org/10.1105/tpc.18.00872

Boavida, L. C., Qin, P., Broz, M., Becker, J. D., & McCormick, S. (2013). Arabidopsis tetraspanins are confined to discrete expression domains and cell types in reproductive tissues and form homo- and heterodimers when expressed in yeast. *Plant Physiology*, *163*, 696–712. https://doi.org/10.1104/pp.113.216598

Borniego, M. L., Molina, M. C., Guiamét, J. J., & Martinez, D. E. (2020). Physiological and proteomic changes in the apoplast accompany leaf senescence in *Arabidopsis*. *Frontiers in Plant Science*, *10*, 1635. https://doi.org/10.3389/fpls.2019.01635

Bose, S., Aggarwal, S., Singh, D. V., & Acharya, N. (2020). Extracellular vesicles: An emerging platform in gram-positive bacteria. *Microbial Cell*, *7*, 312–322. https://doi.org/10.15698/mic2020.12.737

Brusslan, J. A., Bonora, G., Rus-Canterbury, A. M., Tariq, F., Jaroszewicz, A., & Pellegrini, M. (2015). A genome-wide chronological study of gene expression and two histone modifications, H3K4me3 and H3K9ac, during developmental leaf senescence. *Plant Physiology*, *168*, 1246–1261. https://doi.org/10.1104/pp.114.252999

Brusslan, J. A., Rus Alvarez-Canterbury, A. M., Nair, N. U., Rice, J. C., Hitchler, M. J., & Pellegrini, M. (2012). Genome-wide evaluation of histone methylation changes associated with leaf senescence in Arabidopsis. *PLoS ONE*, *7*, e33151. https://doi.org/10.1371/journal.pone.0033151

Buchanan-Wollaston, V., Page, T., Harrison, E., Breeze, E., Lim, P. O., Nam, H. G., Lin, J.-F., Wu, S.-H., Swidzinski, J., Ishizaki, K., & Leaver, C. J. (2005). Comparative transcriptome analysis reveals significant differences in gene expression and signalling pathways between developmental and dark/starvation-induced senescence in Arabidopsis. *The Plant Journal.*, *42*, 567–585. https://doi.org/10.1111/j.1365-313X.2005.02399.x

Cai, Q., Qiao, L., Wang, M., He, B., Lin, F.-M., Palmquist, J., Huang, S.-D., & Jin, H. (2018). Plants send small RNAs in extracellular vesicles to fungal pathogen to silence virulence genes. *Science (1979)*, *360*, 1126–1129. https://doi.org/10.1126/science.aar4142

Chaya, T., Banerjee, A., Rutter, B. D., Adekanye, D., Ross, J., Hu, G., Innes, R. W., & Caplan, J. L. (2024). The extracellular vesicle proteomes of *Sorghum bicolor* and *Arabidopsis thaliana* are partially conserved. *Plant Physiology*, *194*, 1481–1497. https://doi.org/10.1093/plphys/kiad644

Chiu, W.-H., Chandler, J., Cnops, G., Van Lijsebettens, M., & Werr, W. (2007). Mutations in the TORNADO2 gene affect cellular decisions in the peripheral zone of the shoot apical meristem of *Arabidopsis thaliana*. *Plant Molecular Biology*, *63*, 731–744. https://doi.org/10.1007/s11103-006-9105-z

Christie, J. M. (2007). Phototropin blue-light receptors. *Annual Review of Plant Biology*, *58*, 21–45. https://doi.org/10.1146/annurev.arplant.58.032806.103951

Cnops, G., Neyt, P., Raes, J., Petrarulo, M., Nelissen, H., Malenica, N., Luschnig, C., Tietz, O., Ditengou, F., Palme, K., Azmi, A., Prinsen, E., & van Lijsebettens, M. (2006). The *TORNADO1* and *TORNADO2* genes function in several patterning processes during early leaf development in *Arabidopsis thaliana*. *Plant Cell*, *18*, 852–866. https://doi.org/10.1105/tpc.105.040568

Collins, N. C., Thordal-Christensen, H., Lipka, V., Bau, S., Kombrink, E., Qiu, J.-L., Huckelhoven, R., Stein, M., Freialdenhoven, A., Somerville, S., & Schulze-Lefert, P. (2003). SNARE-protein-meidated disease resistance at the plant cell wall. *Nature*, *425*, 973–977. https://doi.org/10.1038/nature02076

Crane, R. A., Cardénas Valdez, M., Castaneda, N., Jackson, C. L., Riley, C. J., Mostafa, I., Kong, W., Chhajed, S., Chen, S., & Brusslan, J. A. (2019). Negative regulation of age-related developmental leaf senescence by the IAOx pathway, PEN1, and PEN3. *Frontiers in Plant Science*, *10*, 1202. https://doi.org/10.3389/fpls.2019.01202

Dai, J., Su, Y., Zhong, S., Cong, L., Liu, B., Yang, J., Tao, Y., He, Z., Chen, C., & Jiang, Y. (2020). Exosomes: Key players in cancer and potential therapeutic strategy. *Signal Transduction and Targeted Therapy*, *5*, 145. https://doi.org/10.1038/s41392-020-00261-0

Fujisaki, K., Kobayashi, S., Tsujimoto, Y., Naito, S., & Ishikawa, M. (2008). Analysis of tobamovirus multiplication in *Arabidopsis thaliana* mutants defective in TOM2A homologues. *Journal of General Virology*, *89*, 1519–1524. https://doi.org/10.1099/vir.0.2008/000539-0

Fujiwara, M., Uemura, T., Ebine, K., Nishimori, Y., Ueda, T., Nakano, A., Sato, M. H., & Fukao, Y. (2014). Interactomics of Qa-SNARE in *Arabidopsis thaliana*. *Plant & Cell Physiology*, *55*, 781–789. https://doi.org/10.1093/pcp/pcu038

Garapati, P., Xue, G.-P., Munné-Bosch, S., & Balazadeh, S. (2015). Transcription factor ATAF1 in Arabidopsis promotes senescence by direct regulation of key chloroplast maintenance and senescence transcriptional cascades. *Plant Physiology*, *168*, 1122–1139. https://doi.org/10.1104/pp.15.00567

Guo, Y., & Gan, S. S. (2012). Convergence and divergence in gene expression profiles induced by leaf senescence and 27 senescence-promoting hormonal, pathological and environmental stress treatments. *Plant, Cell & Environment*, *35*, 644–655. https://doi.org/10.1111/j.1365-3040.2011.02442.x

He, B., Cai, Q., Qiao, L., Huang, C.-Y., Wang, S., Miao, W., Ha, T., Wang, Y., & Jin, H. (2021). RNA-binding proteins contribute to small RNA loading in plant extracellular vesicles. *Nature Plants*, *7*, 342–352. https://doi.org/10.1038/s41477-021-00863-8

He, S., Zhi, F., Min, Y., Ma, R., Ge, A., Wang, S., Wang, J., Liu, Z., Guo, Y., & Chen, M. (2023). The MYB59 transcription factor negatively regulates salicylic acid- and jasmonic acid-mediated leaf senescence. *Plant Physiology*, *192*, 488–503. https://doi.org/10.1093/plphys/kiac589

He, Y., Xu, J., Wang, X., He, X., Wang, Y., Zhou, J., Zhang, S., & Meng, X. (2019). The Arabidopsis pleiotropic drug resistance transporters PEN3 and PDR12 mediate Camalexin secretion for resistance to *Botrytis cinerea*. *Plant Cell*, *31*, 2206–2222. https://doi.org/10.1105/tpc.19.00239

Heard, W., Sklenář, J., Tomé, D. F. A., Robatzek, S., & Jones, A. M. E. (2015). Identification of regulatory and cargo proteins of endosomal and secretory pathways in *Arabidopsis thaliana* by proteomic dissection. *Molecular & Cellular Proteomics*, *14*, 1796–1813. https://doi.org/10.1074/mcp.M115.050286

Jeppesen, D. K., Fenix, A. M., Franklin, J. L., Higginbotham, J. N., Zhang, Q., Zimmerman, L. J., Liebler, D. C., Ping, J., Liu, Q., Evans, R., Fissell, W. H., Patton, J. G., Rome, L. H., Burnette, D. T., & Coffey, R. J. (2019). Reassessment of exosome composition. *Cell*, *177*, 428–445.e18. https://doi.org/10.1016/j.cell.2019.02.029

Jimenez-Jimenez, S., Hashimoto, K., Santana, O., Aguirre, J., Kuchitsu, K., & Cárdenas, L. (2019). Emerging roles of tetraspanins in plant intercellular and inter-kingdom communication. *Plant Signaling & Behavior*, *14*, e1581559. https://doi.org/10.1080/15592324.2019.1581559

Konstantinova, N., Mor, E., Verhelst, E., Nolf, J., Vereecken, K., Wang, F., Van Damme, D., De Rybel, B., & Glanc, M. (2024). A precise balance of TETRASPANIN1/TORNADO2 activity is required for vascular proliferation and ground tissue patterning in Arabidopsis. *Physiologia Plantarum*, *176*, e14182. https://doi.org/10.1111/ppl.14182

Lananna, B. V., & Imai, S. (2021). Friends and foes: Extracellular vesicles in aging and rejuvenation. *FASEB Bioadvances*, *3*, 787–801. https://doi.org/10.1096/fba.2021-00077

Liebana-Jordan, M., Brotons, B., Falcon-Perez, J. M., & Gonzalez, E. (2021). Extracellular vesicles in the fungi kingdom. *International Journal of Molecular Sciences*, *22*, 7221. https://doi.org/10.3390/ijms22137221

Liebsch, D., & Keech, O. (2016). Dark-induced leaf senescence: New insights into a complex light-dependent regulatory pathway. *New Phytologist*, *212*, 563–570. https://doi.org/10.1111/nph.14217

Liu, N., Hou, L., Chen, X., Bao, J., Chen, F., Cai, W., Zhu, H., Wang, L., & Chen, X. (2023). Arabidopsis TETRASPANIN8 mediates exosome secretion and glycosyl inositol phosphoceramide sorting and trafficking. *The Plant Cell*, *36*, 626–641. https://doi.org/10.1093/plcell/koad285

Liu, N.-J., Wang, N., Bao, J.-J., Zhu, H.-X., Wang, L.-J., & Chen, X.-Y. (2020). Lipidomic analysis reveals the importance of GIPCs in *Arabidopsis* leaf extracellular vesicles. *Molecular Plant*, *13*, 1523–1532. https://doi.org/10.1016/j.molp.2020.07.016

Livak, K. J., & Schmittgen, T. D. (2001). Analysis of relative gene expression data using real-time quantitative PCR and the 2(-Delta Delta C(T)) Method. *Methods*, *25*, 402–408. https://doi.org/10.1006/meth.2001.1262

Lu, X., Dittgen, J., Pislewska-Bednarek, M., Molina, A., Schneider, B., Svatos, A., Doubsky, J., Schneeberger, K., Weigel, D., Bednarek, P., & Schulze-Lefert, P. (2015). Mutant allele-specific uncoupling of penetration3 functions reveals engagement of the ATP-binding cassette transporter in distinct tryptophan metabolic pathways. *Plant Physiology*, *168*, 814–827. https://doi.org/10.1104/pp.15.00182

Martinez-Garcia, J. F., Monte, E., & Quail, P. H. (1999) A simple, rapid and quantitative method for preparing Arabidopsis protein extracts for immunoblot analysis. *Plant Journal*, *20*, 251–257. https://doi.org/10.1046/j.1365-313x.1999.00579.x

Porra, R. J., Thompson, W. A., & Kriedemann, P. E. (1989). Determination of accurate extinction coefficients and simultaneous equations for assaying chlorophylls a and b extracted with four different solvents: Verification of the concentration of chlorophyll standards by atomic absorption spectroscopy. *Biochimica et Biophysica Acta*, *975*, 384–394. https://doi.org/10.1016/S0005-2728(89)80347-0

Qi, Y., Tsuda, K., Nguyen, L. V., Wang, X., Lin, J., Murphy, A. S., Glazebrook, J., Thordal-Christensen, H., & Katagiri, F. (2011). Physical association of *Arabidopsis* hypersensitive induced reaction proteins (HIRs) with the immune receptor RPS2. *Journal of Biological Chemistry*, *286*, 31297–31307. https://doi.org/10.1074/jbc.M110.211615

Qin, S., Li, W., Zeng, J., Huang, Y., & Cai, Q. (2024). Rice tetraspanins express in specific domains of diverse tissues and regulate plant architecture and root growth. *The Plant Journal*, *117*, 892–908. https://doi.org/10.1111/tpj.16536

Regente, M., Corti-Monzón, G., Maldonado, A. M., Pinedo, M., Jorrín, J., & de la Canal, L. (2009). Vesicular fractions of sunflower apoplastic fluids are associated with potential exosome marker proteins. *FEBS Letters*, *583*, 3363–3366. https://doi.org/10.1016/j.febslet.2009.09.041

Reimann, R., Kost, B., & Dettmer, J. (2017). TETRASPANINs in plants. *Frontiers in Plant Science*, *8*, 545. https://doi.org/10.3389/fpls.2017.00545

Rubiato, H. M., Liu, M., O'Connell, R. J., & Nielsen, M. E. (2022). Plant SYP12 syntaxins mediate an evolutionarily conserved general immunity to filamentous pathogens. *eLife*, *11*, e73487. https://doi.org/10.7554/eLife.73487

Rutter, B., Rutter, K., & Innes, R. (2017). Isolation and quantification of plant extracellular vesicles. *Bio-Protocol*, *7*, e2533. https://doi.org/10.21769/BioProtoc.2533

Rutter, B. D., & Innes, R. W. (2017). Extracellular vesicles isolated from the leaf apoplast carry stress-response proteins. *Plant Physiology*, *173*, 728–741. https://doi.org/10.1104/pp.16.01253

Stein, M., Diottgen, J., Sanchez-Rodriguez, C., Hou, B.-H., Molina, A., Schulze-Lefert, P., Lipka, V., & Somerville, S. (2006). *Arabidopsis* PEN3/PDR8, an ATP binding cassette transporter, contributes to nonhost resistance to inappropriate pathogens that enter by direct penetration. *Plant Cell Online*, *18*, 731–746. https://doi.org/10.1105/tpc.105.038372

van der Graaff, E., Schwacke, R., Schneider, A., Desimone, M., Flügge, U.-I., & Kunze, R. (2006). Transcription analysis of Arabidopsis membrane transporters and hormone pathways during developmental and induced leaf senescence. *Plant Physiology*, *141*, 776–792. https://doi.org/10.1104/pp.106.079293

Waghmare, S., Lileikyte, E., Karnik, R., Goodman, J. K., Blatt, M. R., & Jones, A. M. E. (2018). SNAREs SYP121 and SYP122 mediate the secretion of distinct cargo subsets. *Plant Physiology*, *178*, 1679–1688. https://doi.org/10.1104/pp.18.00832

Wang, F., Muto, A., Van de Velde, J., Neyt, P., Himanen, K., Vandepoele, K., & Van Lijsebettens, M. (2015). Functional analysis of Arabidopsis TETRASPANIN gene family in plant growth and development. *Plant Physiology*, *169*, 01310.2015. https://doi.org/10.1104/pp.15.01310

Wang, S., He, B., Wu, H., Cai, Q., Ramírez-Sánchez, O., Abreu-Goodger, C., Birch, P. R. J., & Jin, H. (2024). Plant mRNAs move into a fungal pathogen via extracellular vesicles to reduce infection. *Cell Host & Microbe*, *32*, 93–105.e6. https://doi.org/10.1016/j.chom.2023.11.020

Zand Karimi, H., Baldrich, P., Rutter, B. D., Borniego, L., Zajt, K. K., Meyers, B. C., & Innes, R. W. (2022). Arabidopsis apoplastic fluid contains sRNA- and circular RNA–protein complexes that are located outside extracellular vesicles. *Plant Cell*, *34*, 1863–1881. https://doi.org/10.1093/plcell/koac043

Zhang, Z., Feechan, A., Pedersen, C., Newman, M., Qiu, J., Olesen, K. L., & Thordal-Christensen, H. (2007). A SNARE-protein has opposing functions in penetration resistance and defence signalling pathways. *The Plant Journal*, *49*, 302–312. https://doi.org/10.1111/j.1365-313X.2006.02961.x

Zhang, Z., Lenk, A., Andersson, M. X., Gjetting, T., Pedersen, C., Nielsen, M. E., Newman, M.-A., Hou, B.-H., Somerville, S. C., & Thordal-Christensen, H. (2008). A lesion-mimic syntaxin double mutant in *Arabidopsis* reveals novel complexity of pathogen defense signaling. *Molecular Plant*, *1*, 510–527. https://doi.org/10.1093/mp/ssn011

Zhu, T., Sun, Y., & Chen, X. (2022). Arabidopsis tetraspanins facilitate virus infection via membrane-recognition GCCK/RP motif and cysteine residues. *Frontiers in Plant Science*, *13*, 805633. https://doi.org/10.3389/fpls.2022.805633

SUPPORTING INFORMATION

Additional supporting information can be found online in the Supporting Information section at the end of this article.

How to cite this article: Zimmerman, J. A., Verboonen, B., Harrison Hanson, A. P., Arballo, L. R., & Brusslan, J. A. (2024). Arabidopsis apoplast TET8 positively correlates to leaf senescence, and *tet3tet8* double mutants are delayed in leaf senescence. *Plant Direct*, *8*(9), e70006. https://doi.org/10.1002/pld3.70006